

PKA signaling-mediated inhibition of the AIM2 inflammasome is involved in the radioprotective effect of Eleutheroside E

Liangliang Zhang^{1,2}, Changkun Hu^{1,2}, Zekun Wu^{2,3}, Ziqiao Yan^{2,4}, Chengrong Xiao², Xianglin Tang^{2,*}, Zebin Liao^{2,*}, Yue Gao^{1,2,5,*}

¹Tianjin University of Traditional Chinese Medicine, Tianjin, China; ²Department of Pharmaceutical Sciences, Beijing Institute of Radiation Medicine, Beijing, China; ³School of Pharmacy, Guangdong Pharmaceutical University, Guangzhou, Guangdong, China; ⁴Department of Traditional Chinese Medicine, the Sixth Medical Center of Chinese People's Liberation Army (PLA) General Hospital, Beijing, China; ⁵State Key Laboratory of Kidney Diseases, Chinese PLA General Hospital, Beijing, China

Abstract

Objective: To investigate the protective effect and underlying mechanism of Eleutheroside E (EE), derived from *Acanthopanax senticosus*, against γ -ray radiation-induced splenic injury.

Methods: The Cell Counting Kit-8 assay was used to determine the toxicity of the drug. Hematoxylin and eosin, terminal deoxynucleotidyl transferase dUTP nick end-labeling, and live/dead cell double staining assays were used to evaluate the protective effects of EE on the spleen. Immunofluorescence, immunohistochemical, and enzyme-linked immunosorbent assays (ELISA) were used to investigate the underlying mechanisms of EE. Cross-talk between the absent in melanoma 2 (AIM2) inflammasome and the protein kinase A (PKA) signaling pathway was clarified using selective inhibitors.

Results: EE reduced IR-induced splenic injury—the increased apoptosis rates and the levels of γ -H2AX and inflammatory factors in splenic cells were significantly alleviated. ELISA showed that EE reduced the level of interferon- γ (IFN- γ), interleukin-1 β (IL-1 β), interleukin-6 (IL-6), interleukin-18 (IL-18), and tumor necrosis factor- α (TNF- α) in irradiated tissues. The radioprotective effects of EE were mediated by inhibition of the AIM2 inflammasome and stimulation of PKA signaling, in which EE inhibited the increased levels of AIM2, apoptosis-associated speck-like protein containing a CARD (ASC), and cleaved caspase-1 proteins upon ionizing radiation damage but rescued the decreased protein levels in PKA signaling. Suppression of AIM2 signaling was dependent on the activation of PKA signaling by EE treatment.

Conclusions: EE exerts a significant radioprotective effect on the spleen *in vitro* and *in vivo*. Activation of the PKA signaling pathway leads to AIM2 inflammasome inhibition, thereby attenuating radiation-induced DNA damage. This was demonstrated to be the mechanism involved in the radioprotective effects of EE. Thus, EE can be used as a potential radioprotective drug in clinical practice.

Keywords: AIM2 inflammasome, DNA damage, Eleutheroside E, PKA signaling pathway, Radiation damage

Graphical abstract: <http://links.lww.com/AHM/A157>.

Introduction

With the rapid development of nuclear technology, ionizing radiation has been widely used in medical diagnosis, nuclear medicine, and radiation therapy. However, the adverse effects of radiation exposure on radiation-sensitive tissues are of great concern^[1]. In recent years, with the tense nuclear security situation worldwide and rapid development of radiation therapy, research on radiation damage protection drugs has attracted considerable attention.

The spleen is the largest peripheral immune organ in the body and contains many lymphocytes and plays important roles in immune regulation^[2–3]. Because of the high sensitivity of the spleen to radiation, lymphocytes die within a few hours of exposure to ionizing radiation, thus affecting normal hematopoietic and immune functions^[4–5]. Although the body's self-repair mechanisms can mitigate detectable damage, spleen function may already be impaired after irradiation, which can lead to

Liangliang Zhang, Changkun Hu, and Zekun Wu contributed equally to this work.

*Corresponding author. Yue Gao, E-mail: gaoyue@bmi.ac.cn; Zebin Liao, E-mail: 18701832213@163.com; Xianglin Tang, E-mail: tangxianglin@193.com.

Received 26 January 2024 / Accepted 18 February 2025

How to cite this article: Zhang LL, Hu CK, Wu ZK, Yan ZQ, Xiao CR, Tang XL, Liao ZB, Gao Y. PKA signaling-mediated inhibition of the AIM2 inflammasome is involved in the radioprotective effect of Eleutheroside E. *Acupunct Herb Med* 2025;5(4):443–455. DOI: 10.1097/HM9.000000000000152

Copyright © 2025 Tianjin University of Traditional Chinese Medicine. This is an open-access article distributed under the terms of the Creative Commons Attribution-Non Commercial-No Derivatives License 4.0 (CCBY-NC-ND), where it is permissible to download and share the work provided it is properly cited. The work cannot be changed in any way or used commercially without permission from the journal.

a significantly higher risk of mortality from advanced infection-related diseases^[6]. Thus, the development of therapeutic agents to mitigate radiation-induced spleen damage is of great importance.

Eleutheroside E (EE), a phenolic glycoside, is one of the main active ingredients of the traditional Chinese medicinal plant *Acanthopanax senticosus* in the family *Araliaceae* and has various pharmacological effects, such as anti-inflammatory and anti-fatigue effects and enhancement of the adaptive capacity of the organism^[7–9]. EE has therapeutic effects on osteoporosis and plateau pulmonary edema^[10–11]. In addition, it has positive effects on the nervous system, such as enhancement of memory in sleep-deprived mice^[12], alleviation of isoflurane-induced cognitive dysfunction^[13], improvement of intestinal flora^[14], and a protective effect on neural atrophy^[15]. It also has a protective effect on radiation-induced cognitive and memory impairments^[16]; however, whether EE plays a role in protecting the spleen against radiation damage remains unclear. In this study, we found that EE attenuates irradiation-induced damage to lymphocytes and splenic tissues and inhibits absent in melanoma 2 (AIM2) inflammatory signaling by activating the protein kinase A (PKA) signaling pathway, thereby attenuating irradiation-induced cellular DNA damage.

Materials and methods

Chemicals and reagents

EE was purchased from MedChemExpress (Monmouth Junction, NJ, USA). Calcein-acetoxymethyl ester (AM)/propidium iodide (PI) Double Staining Kit was purchased from Dojindo Laboratories (Kumamoto, Japan). Tumor necrosis factor- α (TNF- α), interleukin-6 (IL-6), interleukin-1 β (IL-1 β), interleukin-18 (IL-18), cyclic adenosine monophosphate (cAMP), cAMP response element-binding protein (CREB), and phosphorylated cAMP response element-binding protein (p-CREB) were purchased from Meimian (Jiangsu, China). γ -H2AX (ab81299) was purchased from Abcam (Cambridge, UK). Apoptosis-associated speck-like protein containing a CARD (ASC) (67824S) and AIM2 (63660S) were purchased from Cell Signaling Technology (Danvers, MA, USA). CREB (R381013) and p-CREB (340731) were purchased from Chengdu Zhongneng Biologicals (Chengdu, China). PRKAC α (2798-1-AP) and PRKAC β (12232-1-AP) were purchased from Proteintech (Wuhan, China). Cleaved caspase-1 was purchased from Signalway Antibody (College Park, MD, USA).

Animals and treatments

Six- to 8-week-old C57BL/6J mice were sourced from Beijing Vital River Laboratory Animal Technology Co., Ltd. (Beijing, China), all mice used in this study were male. All animal procedures were approved by the Animal Care and Use Committee of the Animal Center of the Academy (IACUC-DWZX-2021-557). The mice were housed under controlled conditions (temperature: $25 \pm 1^\circ\text{C}$, humidity: 50%–60%, with a 12 h:12h light-dark cycle) and had unrestricted access to a standard rodent diet (American Institute of Nutrition Rodent Diets-93G) and water. After 1 week of acclimatization, the mice were randomly

assigned to one of three groups ($n = 10$): vehicle control group, irradiation control group (12 hours before irradiation and 0.5, 12, 24, and 48 hours after irradiation), and IR + EE groups (12 hours before irradiation and 0.5, 12, 24, and 48 hours after irradiation). Mice in the control group were intraperitoneally injected with oil, whereas other mice were intraperitoneally injected with 30 mg/kg EE (EE dissolved in corn oil).

Irradiation exposure

The ⁶⁰Co γ radiation facility of the Institute of Radiation Medicine, Academy of Military Medical Sciences, Academy of Military Sciences, Beijing, China, was used for the irradiation. Mice were exposed to 5 Gy at a rate of 67.0 ± 0.5 cGy/min.

Cell culture and treatment

AHH-1 cells were obtained from normal adult blood tissue provided by the Department of Pharmaceutical Sciences, Beijing Institute of Radiation Medicine. They were cultured at 37°C with 5% CO₂ until reaching 70% to 80% confluency. EE was administered 12 hours before irradiation at a concentration of 10 $\mu\text{mol/L}$. Cells in both control and experimental groups were subjected to distinct treatments, including specific treatments. All the treated cells were subsequently collected for further experiments.

Calcein-AM/PI staining assay

AHH-1 cells (5×10^5) were seeded into six-well plates and incubated for 24 hours. Each group received its respective treatment. After incubation, cell suspensions were collected and stained with AM/PI dye in the dark. Subsequently, 150 μL of each stained suspension was transferred to a 24-well plate and incubated for 30 minutes. The fluorescence was observed using a fluorescence microscope (Cytation 5; Bio-Tek, Winooski, VT, USA).

Cell Counting Kit-8 (CCK8) assay

The CCK8 assay was used to assess drug toxicity. AHH-1 cells (5×10^3) were seeded into 96-well plates and incubated for 24 hours. Various concentrations of EE (2.5, 5, 10, 20, and 40 $\mu\text{mol/L}$) were added and incubated for 24 and 48 hours. After incubation, the plates were washed with phosphate-buffered saline, and 100 μL of RPMI-1640 containing 10% CCK reagent was added to each well. The plates were then incubated in a CO₂ incubator for 3 hours. The optical density of the different wells was determined at 450 nm using a microplate reader (VICTOR; Perkin Elmer, Waltham, MA, USA) and was used to calculate relative cell viability.

Histopathological examinations of splenic tissues

Splenic tissues were fixed in 4% paraformaldehyde, sectioned, and subjected to a graded alcohol dehydration series. After dehydration, specimens were cleared in xylene, embedded in paraffin, and sectioned into 4 to 6 μm slices. For histological analysis, sections were deparaffinized with xylene and stained with hematoxylin and eosin (H&E).

Immunohistochemical and terminal deoxynucleotidyl transferase dUTP nick end-labeling (TUNEL) assays

After fixation, splenic tissues were cut into 5 μm sections, deparaffinized, and rehydrated using a series of xylene and aqueous alcohol solutions. They were then incubated overnight at 4°C with primary antibodies against AIM2, cleaved caspase-1, ASC, $\gamma\text{-H2AX}$, PKAC α , PKAC β , CREB, and p-CREB. Following incubation with biotin-labeled secondary antibodies and streptavidin-horseradish peroxidase for 50 minutes at room temperature, immunoreactivity was visualized using 3,3'-diaminobenzidine (DAB) and counterstained with hematoxylin. Positive staining localization was analyzed via light microscopy.

Cellular apoptosis in the splenic tissue was assessed using a TUNEL assay kit (Roche, Sigma-Aldrich, St. Louis, MO, USA). Briefly, following dewaxing and hydration, tumor sections were digested with proteinase K for 30 minutes and labeled with a TUNEL reaction mixture for 2 hours at 37°C. The apoptosis index was determined by selecting five positive fields per sample, counting positive cells in each section (400 \times), and calculating the average ratio of positive cells to total cells across the fields.

Enzyme-linked immunosorbent assay (ELISA)

The supernatant fractions of the spleen and AHH-1 cells were analyzed using ELISA kits to measure the levels of interferon- γ (IFN- γ), IL-6, TNF- α , cAMP, CREB, and p-CREB. The absorbance of each sample was measured at 450 nm using a microplate reader (RT-6100; Rayto Life and Analytical Sciences, Shenzhen, China). Standard curves were established using diluted standard solutions to calculate relative targets in the samples. All standards and samples were analyzed in duplicate.

Immunofluorescence assay

AHH-1 cells were cultured in 48-well plates and treated with EE for 24 hours. After washing three times, the cells were fixed with 4% paraformaldehyde for 10 minutes, permeabilized with 0.5% Triton X-100, and blocked with 1% goat serum. They were then incubated overnight at 4°C with the primary antibody $\gamma\text{-H2AX}$ (1:200). Following a 1-hour incubation at room temperature with GoraLite488-conjugated goat anti-rabbit IgG antibody (1:200), nuclei were counterstained with 4',6-diamidino-2-phenylindole. Cell images were captured using a fluorescence microscope (LSM980; Carl Zeiss AG, Oberkochen, Germany).

Immunofluorescence staining

White slices 2 μm thick were prepared, dewaxed, rehydrated, and repaired with 10% fetal bovine serum (FBS). They were then incubated with primary $\gamma\text{-H2AX}$ antibodies for 12 hours at 4°C, followed by incubation with horseradish peroxidase-conjugated secondary antibodies for 1 hour at 37°C. Hoechst33342 nucleating agent was blocked with an anti-fluorescence quencher, and images were captured using a ZEISS LSM980 imager (ZEISS, Oberkochen, Germany).

Statistical analysis

Experimental data were processed and analyzed using GraphPad Prism 8.0.1 statistical analysis software. Statistical significance of the differences between the means was established using analysis of variance. Significance was set at P value ≤ 0.05 .

Results

EE has significant radioprotective effects

To explore the radioprotective effects of EE *in vivo* and *in vitro*, we first determined the cytotoxicity of EE in AHH-1 cells using a CCK8 assay. The results showed that EE was nontoxic, even at a concentration of 40 $\mu\text{mol/L}$ (Figure 1A and B). The protective effect of EE on cells was determined using Calcein-AM/PI staining, which showed that EE significantly reduced cell death after irradiation (Figure 1C). In addition, H&E and TUNEL staining of the spleen were performed to examine the radioprotective effect of EE on the splenic tissues. The results showed that EE significantly attenuated pathological damage to the spleen in mice after whole-body 5 Gy irradiation (Figure 1D), increased the splenic white pulp percentage and the average white pulp area (Figure 1F and G), and reduced the number of apoptotic cells in the spleen of mice after irradiation (Figure 1E and H). These results show that EE significantly improves cell death and splenic tissue damage caused by irradiation and has a significant protective effect against radiation.

EE attenuates irradiation-induced DNA damage

We found that γ -ray irradiation induced a significant upregulation of $\gamma\text{-H2AX}$ expression after 2 h in AHH-1 cells but induced a significant downregulation of $\gamma\text{-H2AX}$ expression in the cells in the EE group (Figure 2A and C), which indicated that EE significantly decreased the expression of $\gamma\text{-H2AX}$, a marker of DNA damage, after irradiation. The results of *in situ* $\gamma\text{-H2AX}$ staining of spleen also showed that EE was able to reduce DNA damage in irradiated tissues (Figure 2B and D).

EE reduces the increased levels of inflammatory factors and inflammasome after irradiation

Radiation leads to increased levels of inflammatory factors in the body. Through ELISA, we found that EE significantly reduced the levels of IFN- γ , IL-1 β , IL-6, IL-18, and TNF- α in cells and tissues 24 and 72 hours after irradiation (Figure 3A–J), which reduced the inflammatory response of the organism. Immunohistochemical experiments further revealed that EE attenuated the upregulation of AIM2, cleaved caspase-1, and ASC in irradiated tissues (Figure 3K–N) and reduced the increase in inflammatory levels in irradiated tissues.

Radioprotective effects of EE are dependent on the AIM2 inflammasome

Previous studies have shown that EE can exert protective effects against high-altitude pulmonary edema by inhibiting the inflammasome and reducing pyroptosis^[11].

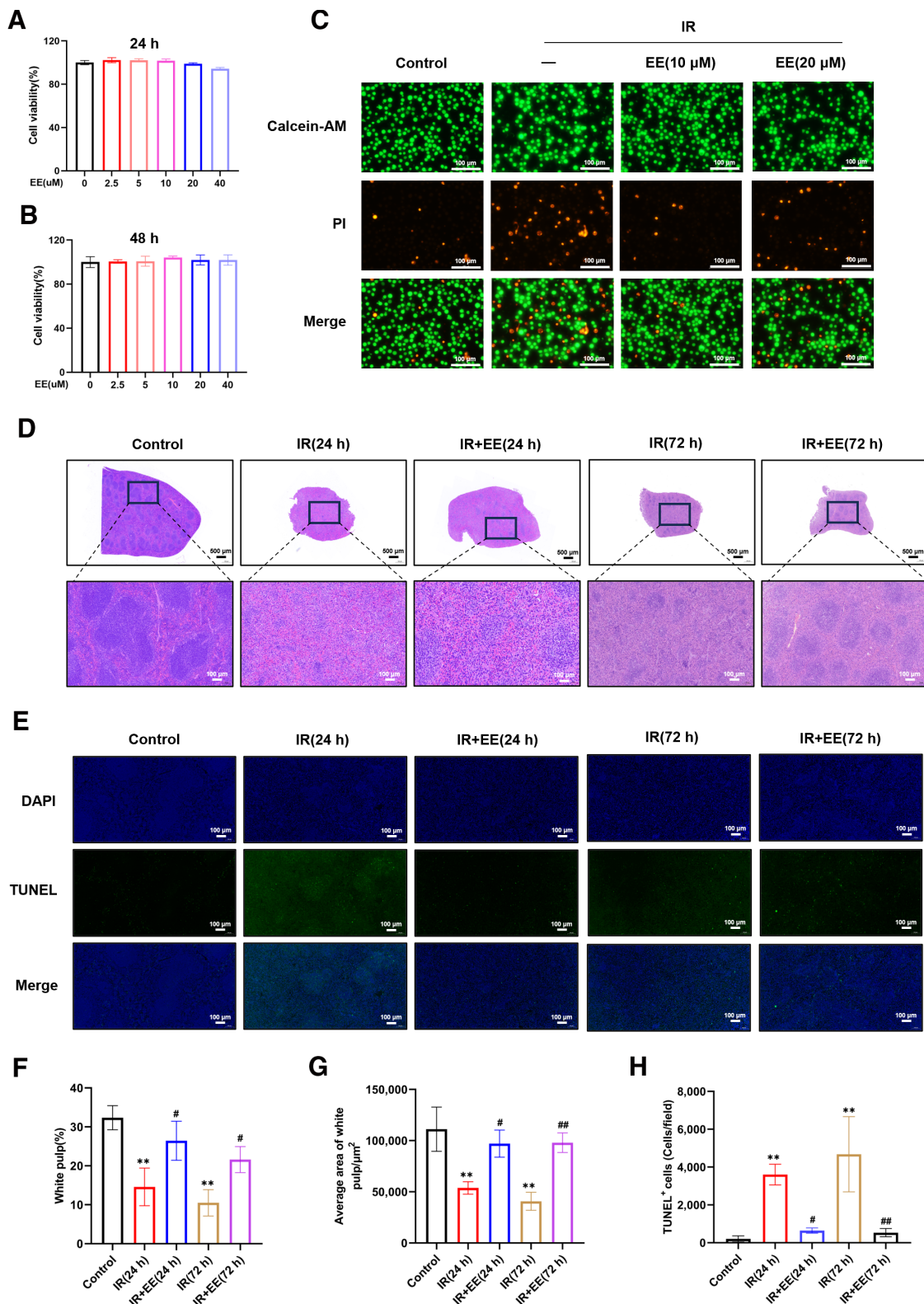


Figure 1. EE exerts significant radioprotective effects. (A) CCK8 assay was used to evaluate drug toxicity 24h after drug administration. (B) CCK8 assay was used to evaluate drug toxicity 48h after drug administration. (C) Calcein-AM/PI assay was used to examine the cytoprotective effect of EE after 5 Gy irradiation. (D) H&E staining was used to examine the protective effect of EE on spleen. (E) Protective effect of EE on the spleen determined using TUNEL staining. (F) Statistics on the percentage of H&E-stained white pulp in the spleen. (G) Mean white pulp area of H&E staining in the spleen. (H) Number of TUNEL-positive cells in the spleen. ***P* < 0.01 vs. control group; #*P* < 0.05, ##*P* < 0.01 vs. IR group. AM: Acetoxymethyl ester; CCK8: Cell Counting Kit-8; DAPI: 4',6-diamidino-2-phenylindole; EE: Eleutheroside E; H&E: Hematoxylin and eosin; IR: Irradiation; PI: Propidium iodide; TUNEL: Terminal deoxynucleotidyl transferase dUTP nick end-labeling.

To confirm whether the radioprotective effect of EE was dependent on the AIM2 inflammasome, we used the AIM2 inhibitor poly(da:dt). The results showed that splenic

radiation damage in mice was exacerbated upon treatment with the AIM2 inhibitor compared with the pathologic splenic damage in the EE radiation administration

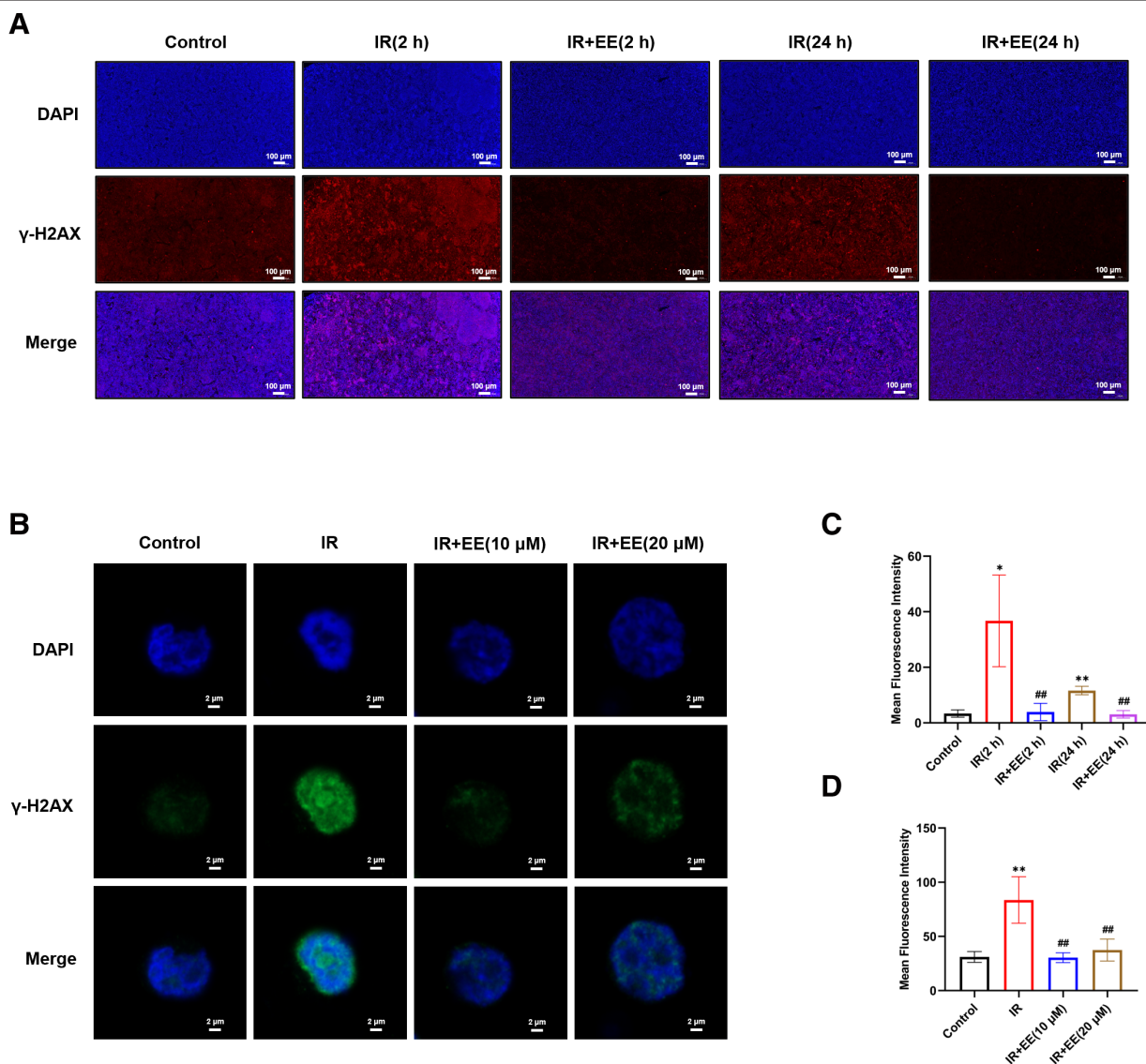


Figure 2. EE attenuates irradiation-induced DNA damage. (A) Tissue immunofluorescence detection of splenic γ -H2AX expression 2 and 24 h after irradiation. (B) Detection of splenic γ -H2AX expression using cellular immunofluorescence 2 h after irradiation. (C) Mean fluorescence intensity statistics of immunofluorescence spleen staining. (D) Mean fluorescence intensity statistics of immunofluorescence cell staining. * $P < 0.05$, ** $P < 0.01$ vs. control group; ## $P < 0.01$ vs. IR group. DAPI: 4',6-diamidino-2-phenylindole; EE: Eleutheroside E; IR: Irradiation.

group (Figure 4A and B). The results of TUNEL staining of the spleen also showed that EE attenuated splenic apoptosis, which was exacerbated by AIM2 inhibitor treatment (Figure 4C and D). Next, we investigated γ -H2AX expression in cells and tissues after treatment with AIM2 inhibitors. The results of tissue immunohistochemical staining and cellular immunofluorescence showed that EE could not decrease γ -H2AX expression in tissues and cells after treatment with the inhibitors (Figure 4E–H). Finally, the radioprotective effect of EE was investigated using the Calcein-AM/PI cell double staining assay in the presence of the AIM2 inhibitor, which also showed that EE did not exert radioprotective effects on the cells upon treatment with the AIM2 inhibitor (Figure 4I and J).

EE significantly alters PKA signaling after irradiation

ELISA experiments revealed that EE significantly upregulated cAMP, CREB, and p-CREB in the PKA

signaling pathway in cells and tissues after irradiation (Figure 5A–H). Immunohistochemical staining was further used to examine the expression of PKAC α , PKAC β , CREB, and p-CREB in tissues, and the results showed that EE upregulated PKAC α , PKAC β , CREB, and p-CREB in irradiated tissues (Figure 5I–M). This indicates that EE activates the PKA signaling pathway.

Radioprotective effects of EE are dependent on the PKA signaling pathway

We verified the mechanism of radioprotection by EE using PKA signaling pathway inhibitors H-8 dihydrochloride and PKI-(6-22)-amide trifluoroacetic acid (TFA). The number of cell deaths was determined using the Calcein-AM/PI cell double staining assay, which showed no significant difference in the number of cell deaths between the PKA signaling pathway inhibitor group and the radiation control group at 24 and 72 hours after

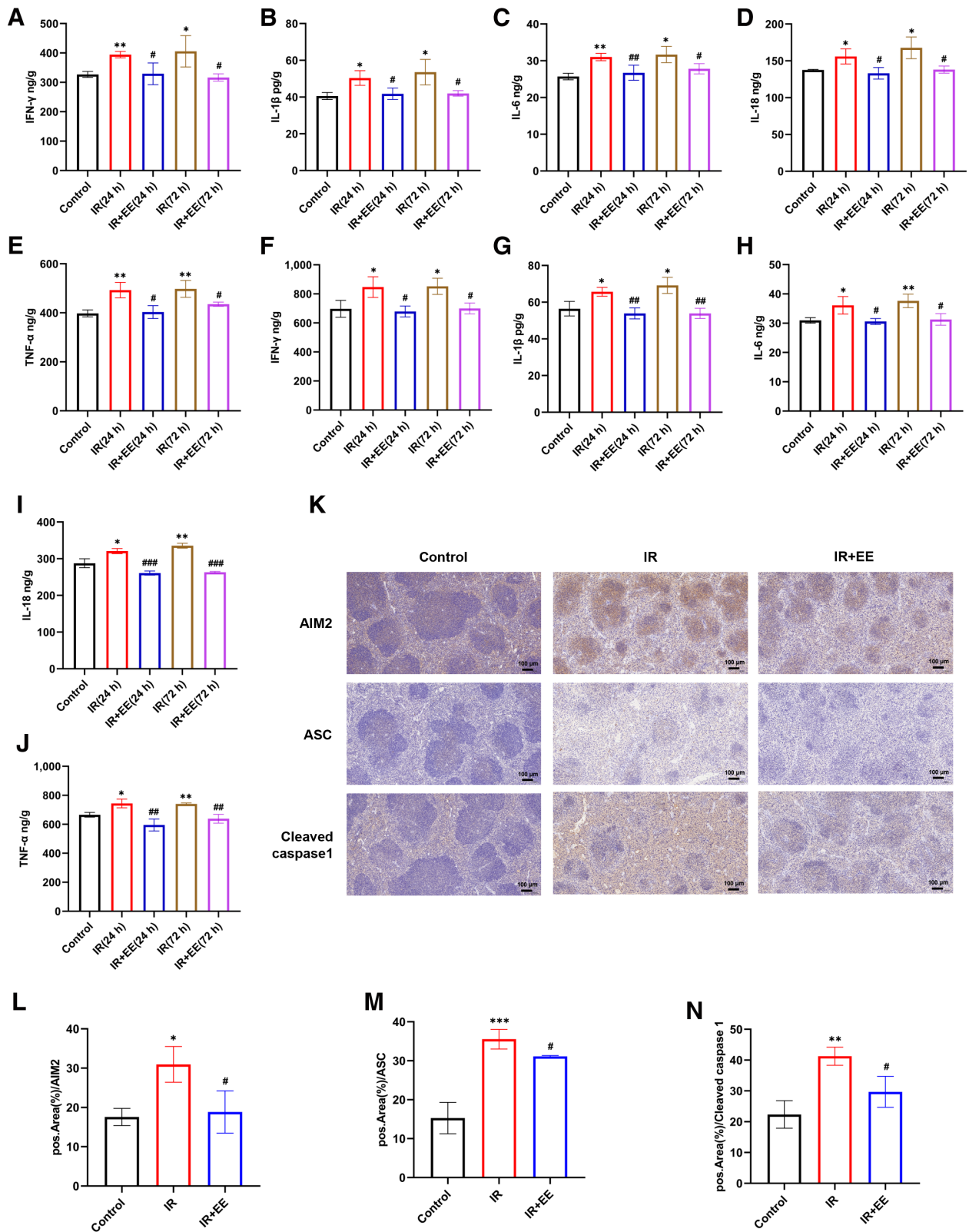


Figure 3. EE reduces the increased levels of inflammatory factors and inflammasome after irradiation. (A–E) ELISA was performed to determine cellular IFN-γ (A), IL-1 β (B), IL-6 (C), IL-18 (D), and TNF-α (E) expression. (F–J) ELISA was performed to determine IFN-γ (F), IL-1 β (G), IL-6 (H), IL-18 (I), and TNF-α (J) expression in tissues. (K) Immunohistochemical detection of AIM2, ASC, and cleaved caspase-1 expression in the tissues. (L) Statistics of AIM2-positive regions in the spleen. (M) Statistics of ASC-positive regions in the spleen. (N) Statistics of cleaved caspase-1-positive regions in the spleen. * $P < 0.05$, ** $P < 0.01$, *** $P < 0.001$ vs. control group; # $P < 0.05$, ## $P < 0.01$, ### $P < 0.001$ vs. IR group. AIM2: Absent in melanoma 2; ASC: Apoptosis-associated speck-like protein containing a CARD; EE: Eleutheroside E; ELISA: Enzyme-linked immunosorbent assay; IFN: Interferon; IL: Interleukin; IR: Irradiation; TNF: Tumor necrosis factor.

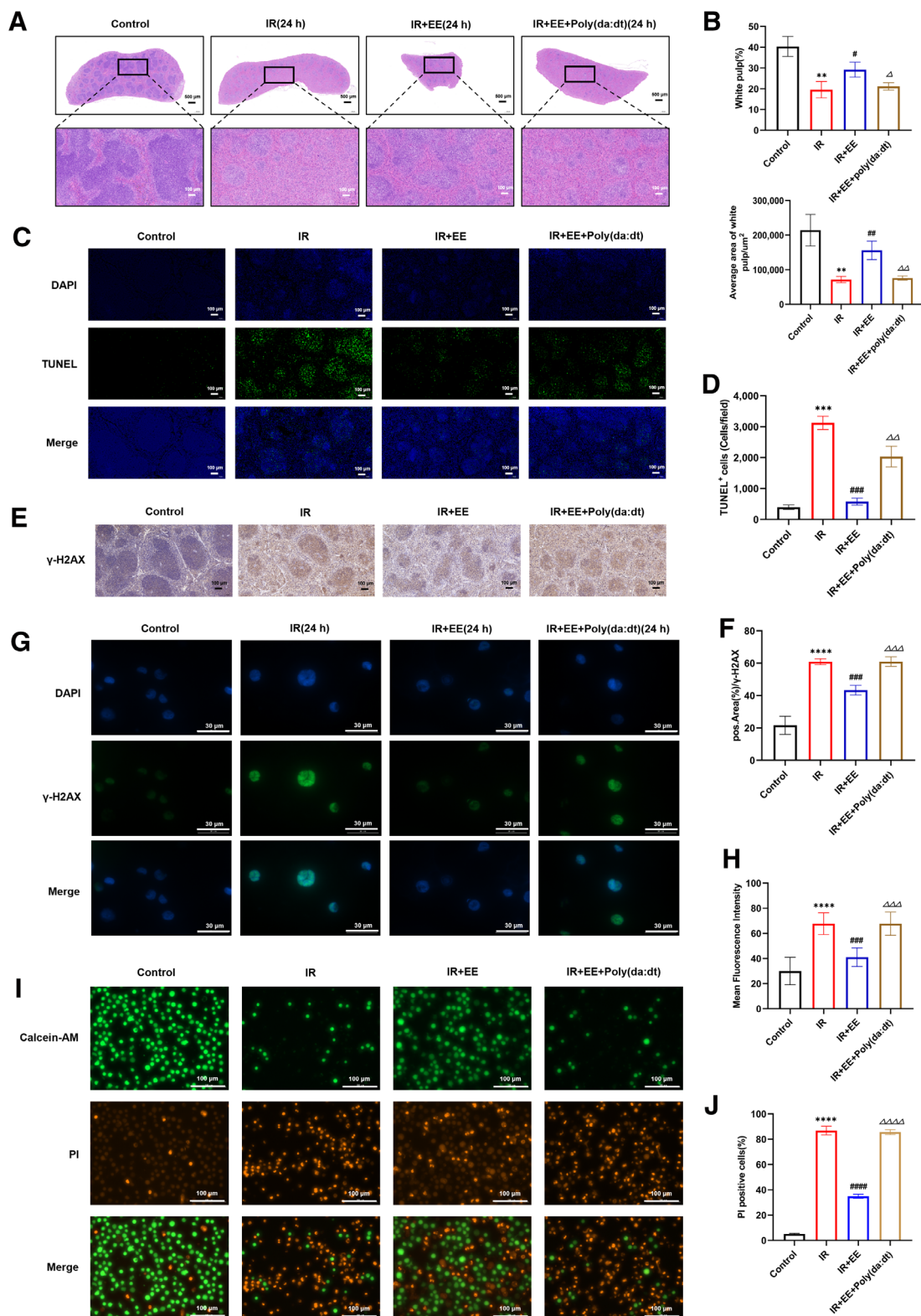


Figure 4. Radioprotective effects of EE are dependent on the AIM2 inflammasome. (A) Detection of pathological splenic injury after treatment with AIM2 inhibitors. (B) The percentage of white pulp and the mean area of white pulp in the spleen. (C) Detection of apoptosis in splenocytes after treatment with AIM2 inhibitors. (D) Number of TUNEL-positive cells in the spleen. (E) Detection of γ-H2AX expression in spleen after treatment with an AIM2 inhibitor. (F) Statistics of γ-H2AX expression in tissues. (G) Detection of cellular γ-H2AX expression after treatment with AIM2 inhibitors. (H) Mean fluorescence intensity statistics of cellular γ-H2AX. (I) AHH-1 cell death after irradiation detected via a Calcein-AM/PI assay using an AIM2 inhibitor. (J) PI-positive cell count. ** $P < 0.01$, *** $P < 0.001$, **** $P < 0.0001$ vs. control group; # $P < 0.05$, ## $P < 0.01$, ### $P < 0.001$, #### $P < 0.0001$ vs. IR group; Δ $P < 0.05$, ΔΔ $P < 0.01$, ΔΔΔ $P < 0.001$, ΔΔΔΔ $P < 0.0001$ vs. IR + EE group. AIM2: Absent in melanoma 2; AM: Acetoxymethyl ester; DAPI: 4',6-diamidino-2-phenylindole; EE: Eleutheroside E; IR: Irradiation; PI: Propidium iodide; TUNEL: Terminal deoxynucleotidyl transferase dUTP nick end-labeling.

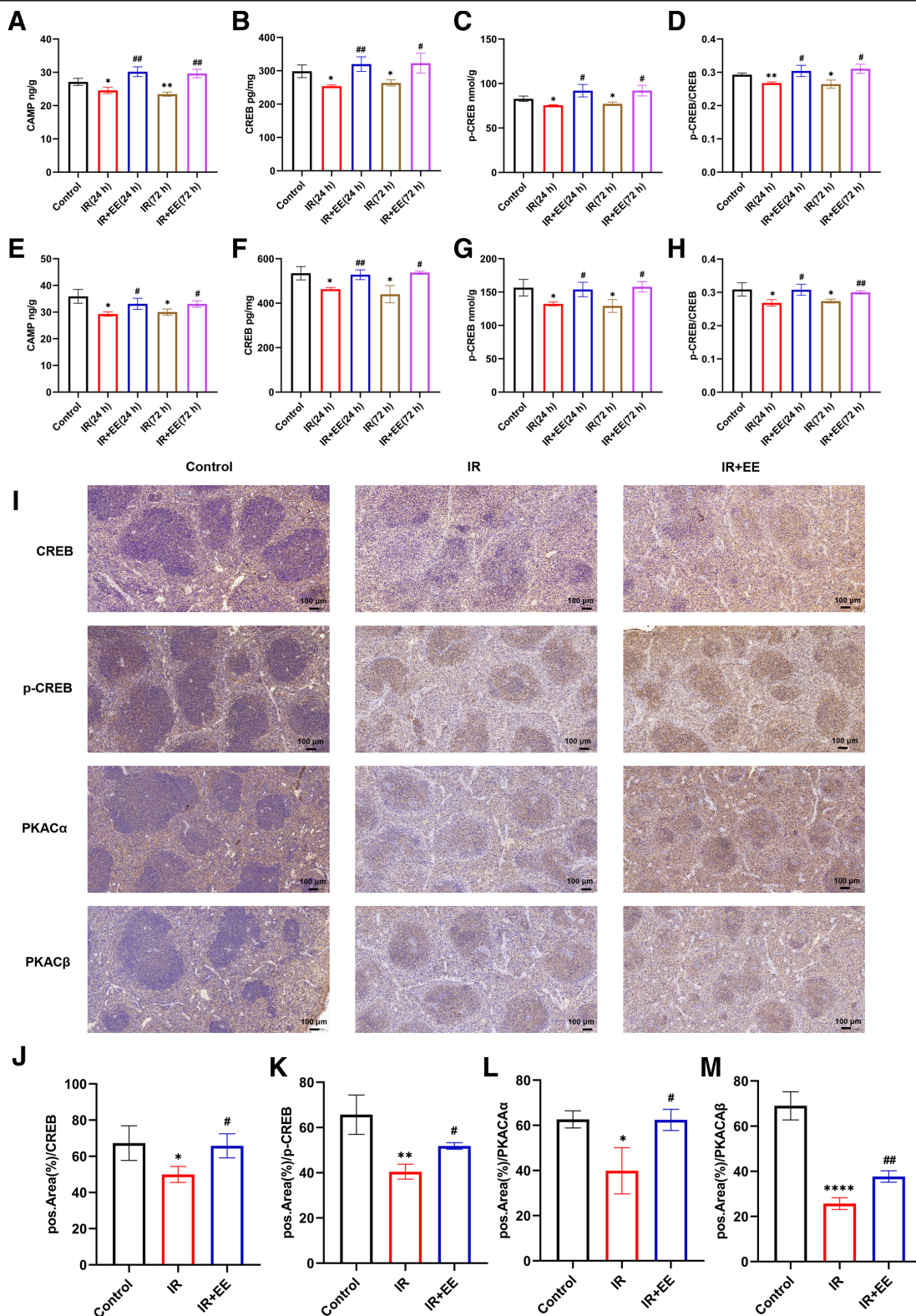


Figure 5. EE significantly alters PKA signaling after irradiation. (A) ELISA was performed to determine cellular cAMP expression. (B) ELISA was performed to determine cellular CREB expression. (C) ELISA was performed to determine cellular p-CREB expression. (D) ELISA was performed to determine cellular p-CREB/CREB expression. (E) ELISA was performed to determine cAMP expression in tissues. (F) ELISA was performed to determine CREB expression in tissues. (G) ELISA was performed to determine p-CREB expression in tissues. (H) ELISA was performed to determine p-CREB/CREB expression in tissues. (I) Immunohistochemical detection of CREB, p-CREB, PKACA α , and PKACA β expression in splenic tissues. (J) Statistics of CREB-positive regions in the spleen. (K) Statistics of p-CREB-positive regions in the spleen. (L) Statistics of PKACA α -positive regions in the spleen. (M) Statistics of PKACA β -positive regions in the spleen. * $P < 0.05$, ** $P < 0.01$, **** $P < 0.0001$ vs. control group; # $P < 0.05$, ## $P < 0.01$ vs. IR group. cAMP: Cyclic adenosine monophosphate; CREB: cAMP response element-binding protein; EE: Eleutheroside E; ELISA: Enzyme-linked immunosorbent assay; IR: Irradiation; p-CREB: Phosphorylated cAMP response element-binding protein; PKA: Protein kinase A; PKACA α : Protein kinase A catalytic subunit α .

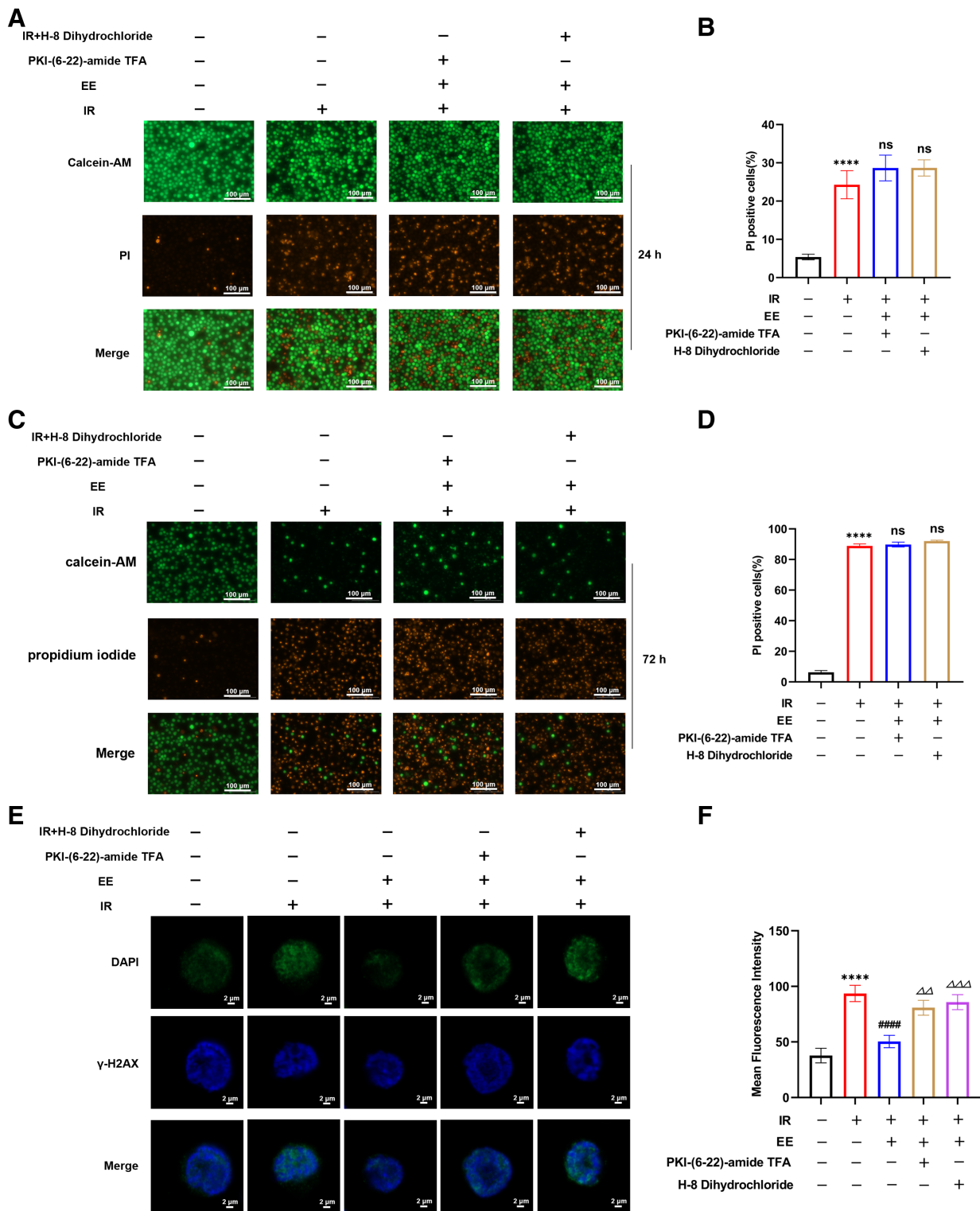


Figure 6. Radioprotective effects of EE are dependent on the PKA signaling pathway. (A) Radioprotective effect of EE 24h post-irradiation determined using a Calcein-AM/PI assay after treatment with PKA inhibitors. (B) Number of PI-positive cells. (C) Radioprotective effect of EE 72h post-irradiation determined using a Calcein-AM/PI assay after treatment with PKA inhibitors. (D) Number of PI-positive cells. (E) Detection of cellular γ -H2AX expression 2h after irradiation using immunofluorescence staining after treatment with PKA inhibitors. (F) Mean fluorescence intensity statistics of cell immunofluorescence staining. **** $P < 0.0001$ vs. control group; #### $P < 0.0001$ vs. IR group; $\Delta\Delta P < 0.01$, $\Delta\Delta\Delta P < 0.001$ vs. IR + EE group. AM: Acetoxymethyl ester; DAPI: 4',6-diamidino-2-phenylindole; EE: Eleutheroside E; IR: Irradiation; PI: Propidium iodide; PKA: Protein kinase A; TFA: Trifluoroacetic acid.

irradiation (Figure 6A–D). Immunofluorescence staining results showed no significant difference in γ -H2AX foci after treatment with the PKA pathway inhibitors compared with the irradiated group, whereas a significant

increase was observed in the irradiated plus EE group (Figure 6E and F). This suggests that the radioprotective effect of EE is also associated with the activation of the PKA pathway.

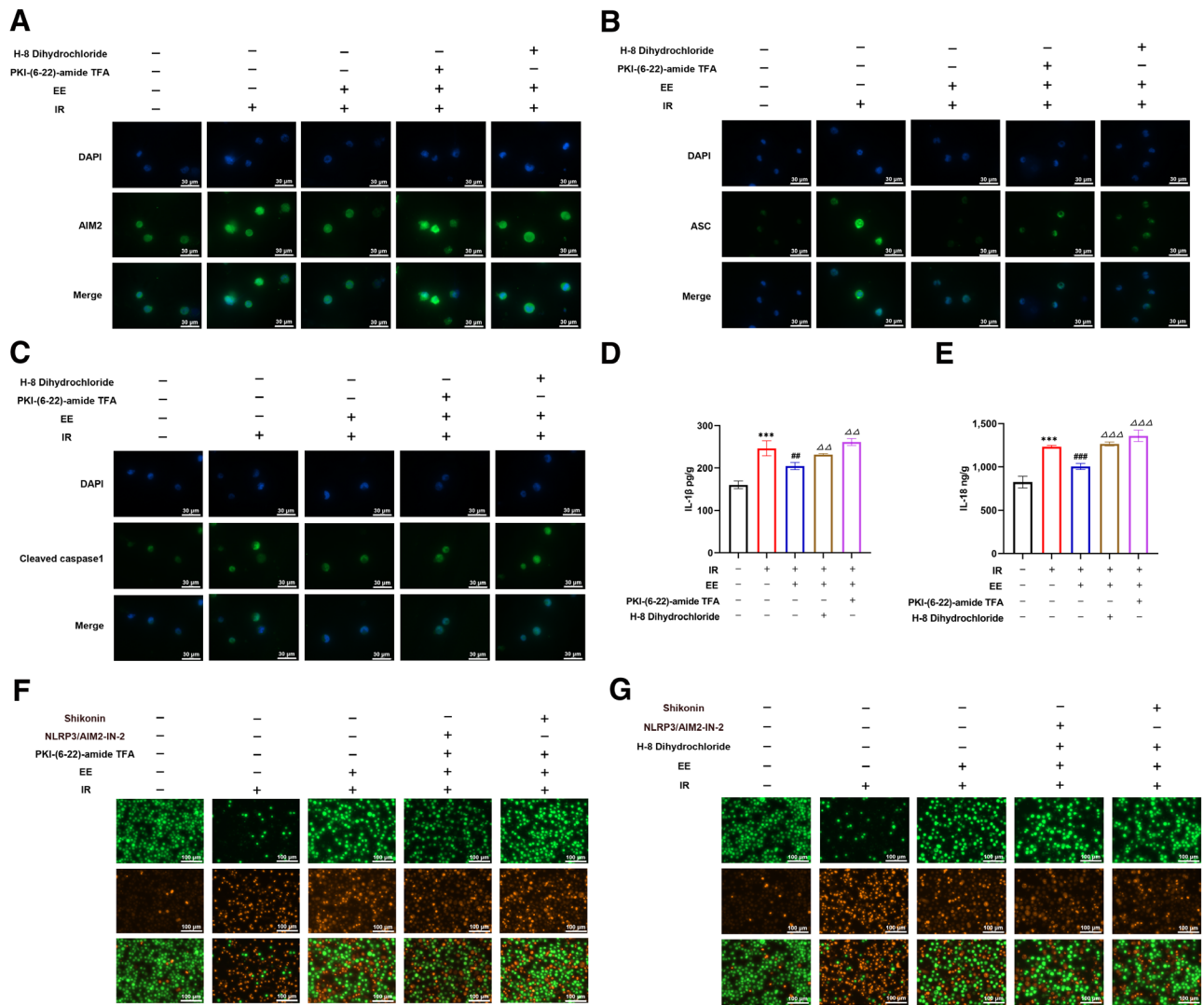


Figure 7. Inhibition of the AIM2 inflammasome by EE via the PKA pathway. (A) Detection of AIM2 expression in cells using immunofluorescence staining after administration of PKA inhibitors. (B) Detection of ASC expression in cells using immunofluorescence staining after administration of PKA inhibitors. (C) Detection of cleaved caspase-1 expression in cells using immunofluorescence staining after administration of PKA inhibitors. (D) Detection of IL-1 β expression in cells using ELISA after administration of PKA inhibitors. (E) Detection of IL-18 expression in cells using ELISA after administration of PKA inhibitors. (F–G) Radioprotective effects of EE determined using a Calcein-AM/PI assay after concomitant administration of PKA and AIM2 inhibitors. *** $P < 0.001$ vs. control group; ## $P < 0.01$, ### $P < 0.001$ vs. IR group; $\Delta\Delta P < 0.01$, $\Delta\Delta\Delta P < 0.001$ vs. IR + EE group. AIM2: Absent in melanoma 2; AM: Acetoxymethyl ester; ASC: Apoptosis-associated speck-like protein containing a CARD; DAPI: 4',6-diamidino-2-phenylindole; EE: Eleutheroside E; ELISA: Enzyme-linked immunosorbent assay; IL: Interleukin; IR: Irradiation; NLRP3: NOD-like receptor family pyrin domain containing 3; PI: Propidium iodide; PKA: Protein kinase A.

Inhibition of the AIM2 inflammasome by EE via the PKA pathway

To further validate the reciprocal regulation of the PKA pathway and the AIM2 inflammasome, we used the PKA signaling pathway inhibitors H-8 dihydrochloride and PKI-(6-22)-amide TFA and the AIM2 inflammatory inhibitors NOD-like receptor family pyrin domain containing 3 (NLRP3)/AIM2-IN-2 and shikonin to validate the radioprotective mechanism of EE. We first used EE in the presence of PKA pathway inhibitors to detect the expression of the AIM2 inflammasome and inflammatory factors after irradiation. Immunofluorescence staining results showed that under inhibition of the PKA pathway, EE could not reduce the expression levels of AIM2, ASC, and cleaved caspase-1 in the irradiated AIM2 inflammasome (Figure 7A–C). The ELISA results also showed that IL-1 β and IL-18 were significantly upregulated in the PKA pathway inhibitor group

compared with the EE administration group (Figure 7D and E). These suggest that the AIM2 inflammasome and inflammatory factors were significantly upregulated in the AIM2 inflammatory group. AIM2 and PKA inhibitors were used to verify this regulatory relationship. Under the inhibition of the PKA pathway and further inhibition of AIM2, the results of Calcein-AM/PI cell double staining showed that EE significantly reduced the number of cell deaths after irradiation (Figure 7F and G), indicating that the radioprotective effect of EE was exerted by activating the PKA pathway and inhibiting the AIM2 inflammatory vesicles to exert radioprotective effects.

Discussion

The spleen is an important part of the immune system and is the primary source of lymphocytes^[17]. Studies

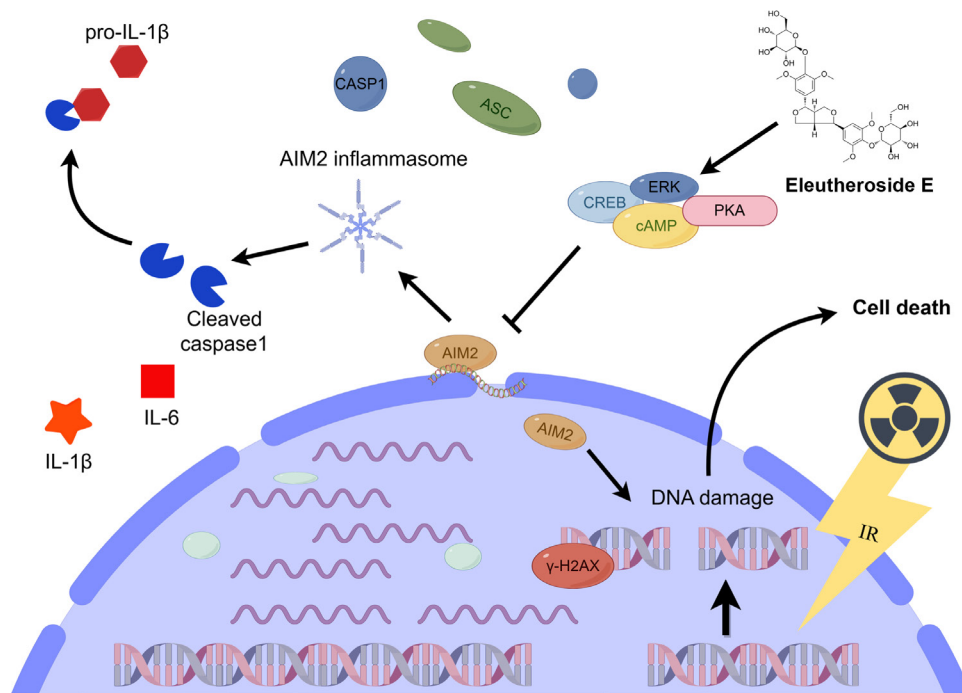


Figure 8. Diagram of the mechanism of action of EE for radiation protection. AIM2: Absent in melanoma 2; cAMP: Cyclic adenosine monophosphate; CREB: cAMP response element-binding protein; EE: Eleutheroside E; ERK: Extracellular signal-regulated kinase; IL: Interleukin; IR: Irradiation; PKA: Protein kinase A.

have shown that radiation disrupts the balance of oxidative stress in the spleen tissues, blocks cell proliferation, promotes apoptosis, and reduces the number of lymphocytes and affects their structure and function, ultimately leading to a decline in immune function and a series of complications^[18–19]. In the present study, we found that EE significantly reduced splenic damage after irradiation, decreased the apoptosis of splenic cells, and reduced irradiation-induced DNA damage.

Ionizing radiation is a high-energy radiation that produces intermediate ions and free radicals that damage genetic material and lead to genomic instability^[20–22]. The energy generated by IR can lead to DNA damage in cells through direct action, triggering DNA single-strand^[23] and double-strand breaks^[24], chromosomal rearrangements^[25], and other related processes. It can also lead to DNA damage through indirect effects, in which the energy generated by radiation is absorbed by intracellular water molecules, leading to the generation of reactive oxygen species (ROS) and other related factors, which in turn leads to cellular stress and ultimately, DNA damage^[26–27]. The AIM2 inflammasome plays a key role in the DNA damage process^[28–29] and is composed of AIM2 and ASC, which can recognize double-stranded DNA breaks (DSBs) caused by IR and chemotherapeutic drugs^[30–31]. Under the effect of radiation, AIM2 enters the nucleus and localizes to DSB foci, forming speckles and recruiting ASC. This leads to caspase-1 activation, which mediates inflammasome activation and cell death^[32]. Thus, the mechanism of action of EE may be through/via the inhibition of the AIM2 inflammasome. Our study confirms that EE inhibits irradiation-induced AIM2 inflammatory activation and that the use of a specific agonist counters the effect of EE on irradiation-induced DNA damage.

Previous studies reported that EE can improve radiation-induced cognitive deficits and protect against radiation-induced neurological damage and that its mechanism of action is closely related to the cAMP/PKA signaling pathway^[33]. The cAMP/PKA signaling pathway is involved in the regulation of working memory and neuronal differentiation, reward, and learning^[34–36]. In addition, PKA can activate CREBs through phosphorylation, and activated CREBs are associated with long-term synaptic plasticity, learning, and memory^[37]. In addition, the activation of PKA/CREB signaling can promote the expression of anti-inflammatory genes, which can exert anti-inflammatory effects^[38–40]. Considering the ability of EE to inhibit inflammasomes and reduce the levels of inflammatory factors after irradiation, we hypothesized that the PKA pathway is a key mechanism that mediates the action of EE. We showed that EE activated key molecules in the PKA signaling pathway, and further validation using PKA pathway inhibitors revealed that the radioprotective effects of EE were dependent on the PKA pathway.

Numerous studies have demonstrated the regulatory relationship between PKA and inflammatory pathways. For example, the activation of PKA reduces NLRP3 inflammatory activation and retinal inflammation^[41], inhibits NLRP3 inflammatory activation, and attenuates inflammatory responses by regulating PKA signaling^[42]. However, the role of PKA in regulating the AIM2 inflammasome has not yet been reported. To explore the regulatory role of the PKA pathway in AIM2, we used PKA pathway inhibitors and detected AIM2 inflammatory expression under the inhibition of the PKA pathway and found that EE could not attenuate cellular inflammatory expression. Further inhibition of the AIM2 inflammasome under

PKA inhibition reversed the radioprotective effects of EE. The results showed that EE did not reduce the expression of cellular inflammasomes upon PKA inhibition. Finally, EE inhibited the AIM2 inflammasome by activating PKA, which attenuated radiation-induced DNA damage.

In this study, we investigated the protective effects of EE against radiation-induced spleen damage, cell apoptosis, and DNA damage. However, there are several limitations: although we explored the inhibition of the AIM2 inflammasome and activation of the PKA signaling pathway as potential mechanisms underlying EE's protective effects, the depth of these mechanistic studies was limited. Future research should employ more refined molecular biology techniques to thoroughly elucidate the mechanisms of EE. Besides, this study primarily utilized animal models, and the clinical relevance of the findings remains to be further validated. Future studies should consider preclinical and clinical trials to assess the efficacy and safety of EE in clinical applications. Despite these limitations, our study provides valuable preliminary data on the potential application of EE in mitigating radiation-induced spleen damage. Future research should address these limitations to further validate the therapeutic effects and mechanisms of EE.

Conclusion

In conclusion, our study found that EE can reduce splenic damage caused by radiation exposure and that its protective mechanism involves activation of the PKA pathway to inhibit the AIM2 inflammasome, which in turn reduces radiation-induced DNA damage (Figure 8). Thus, EE exerts a protective effect against radiation damage, suggesting its potential value as a candidate drug for radiation protection.

Conflict of interest statement

Yue Gao is the editorial board member of this journal and other authors declare no conflict of interest.

Funding

This work was financially supported by the National Natural Science Foundation of China (82103776, Zebin Liao; 82192911, Yue Gao), and innovation Team and Talents Cultivation Program of National Administration of Traditional Chinese Medicine (ZYYCXTD-D-202207, Yue Gao).

Author contributions

Yue Gao and Zebin Liao designed the project. Liangliang Zhang, Changkun Hu, and Zekun Wu performed most of the experiments and analyzed data. Liangliang Zhang and Changkun Hu performed molecular biology and cell biology experiments and conducted data curation and formal analysis. Liangliang Zhang and Zekun Wu performed the animal experiments. Liangliang Zhang and Zebin Liao wrote the manuscript. Yue Gao and Xianglin Tang contributed to the manuscript editing.

Ethical approval of studies and informed consent

Not applicable.

Acknowledgments

None.

Data availability

Data and materials are available upon request to the corresponding author.

References

- [1] Shao S, Gao Y. Traditional Chinese medicine: an important coping strategy with challenges of radiation injury. *Acupunct and Herb Med.* 2024;4(4):427–435.
- [2] Zeng Z, Liu Z, Li J, et al. Baseline splenic volume as a biomarker for clinical outcome and circulating lymphocyte count in gastric cancer. *Front Oncol* 2023;12:1065716.
- [3] Niu HG, Tang ZY, et al. Formulations of traditional Chinese medicine for the prevention and treatment of radiation-induced injury. *Acupunct and Herb Med.* 2024;4(4):463–474.
- [4] Hollingsworth BA, Aldrich JT, Case CM, et al. Immune dysfunction from radiation exposure. *Radiat Res* 2023;200(4):396–416.
- [5] Heylmann D, Rödel F, Kindler T, et al. Radiation sensitivity of human and murine peripheral blood lymphocytes, stem and progenitor cells. *Biochim Biophys Acta* 2014;1846(1):121–129.
- [6] Weil BR, Madenci AL, Liu Q, et al. Late infection-related mortality in splenic survivors of childhood cancer: a report from the childhood cancer survivor study. *J Clin Oncol* 2018;36(16):1571–1578.
- [7] Cheng J, Qiu L, Ahmad N, et al. Screening of anti-fatigue active ingredients of *Eleutherococcus senticosus* via spectrum-effect relationship based on factor analysis and LC-MS/MS. *Nat Prod Res* 2023;37(24):4144–4155.
- [8] Li H, Han R, Yong F, et al. The protective effect of Eleutheroside E against the mechanical barrier dysfunction triggered by lipopolysaccharide in IPEC-J2 cells. *Res Vet Sci* 2022;154:1–7.
- [9] Liu YC, Yang YJ, Chen MS, et al. Anti-inflammatory and analgesic effects of eleutheroside E in alcoholic beverage. *J Biol Regul Homeost Agents* 2019;33(6):1815–1821.
- [10] Zhou T, Zhou Y, Ge D, et al. Decoding the mechanism of Eleutheroside E in treating osteoporosis via network pharmacological analysis and molecular docking of osteoclast-related genes and gut microbiota. *Front Endocrinol (Lausanne)* 2023;14:1257298.
- [11] Hu CK, Wu ZK, Zhang LL, et al. Isofraxidin alleviated radiation-induced testicular damage via the Nrf2/HO-1-NLRP3/ASC Axis. *Acupunct and Herb Med.* 2024;44:457–486.
- [12] Huang LZ, Wei L, Zhao HF, et al. The effect of Eleutheroside E on behavioral alterations in murine sleep deprivation stress model. *Eur J Pharmacol* 2011;658(2-3):150–155.
- [13] Lu X, Xiao-Qing C. Eleutheroside E attenuates isoflurane-induced cognitive dysfunction by regulating the α 7-nAChR-NMDAR pathway. *Neuroreport* 2019;30(3):188–194.
- [14] Song C, Duan F, Ju T, et al. Eleutheroside E supplementation prevents radiation-induced cognitive impairment and activates PKA signaling via gut microbiota. *Commun Biol* 2022;5(1):680.
- [15] Jia A, Zhang Y, Gao H, et al. A review of *Acanthopanax senticosus* (Rupr and Maxim.) harms: from ethnopharmacological use to modern application. *J Ethnopharmacol* 2020;268:113586.
- [16] Song C, Li S, Duan F, et al. The therapeutic effect of *acanthopanax senticosus* components on radiation-induced brain injury based on the pharmacokinetics and neurotransmitters. *Molecules* 2022;27(3):1106.
- [17] Zaitoun MMA, Basha MAA, Elsayed SB, et al. Comparison of three embolic materials at partial splenic artery embolization for hypersplenism: clinical, laboratory, and radiological outcomes. *Insights Imaging* 2021;12(1):85.
- [18] Zhang H, Cheng Y, Luo X, et al. Protective effect of procyanidins extracted from the lotus seedpod on immune function injury induced by extremely low frequency electromagnetic field. *Biomed Pharmacother* 2016;82:364–372.
- [19] Yi J, Chen C, Liu X, et al. Radioprotection of EGCG based on immunoregulatory effect and antioxidant activity against 60Co γ radiation-induced injury in mice. *Food Chem Toxicol* 2019;135:111051.

- [20] Chen Y, Cui J, Gong Y, et al. MicroRNA: a novel implication for damage and protection against ionizing radiation. *Environ Sci Pollut Res Int* 2021;28(13):15584–15596.
- [21] Baulch JE. Radiation-induced genomic instability, epigenetic mechanisms and the mitochondria: a dysfunctional ménage à trois? *Int J Radiat Biol* 2018;95(4):516–525.
- [22] Fang L, Li J, Li W, et al. Assessment of genomic instability in medical workers exposed to chronic low-dose x-rays in Northern China. *Dose Response* 2019;17(4):1559325819891378.
- [23] Abbotts R, Wilson DM 3rd. Coordination of DNA single strand break repair. *Free Radic Biol Med* 2017;107:228–244.
- [24] Borrego-Soto G, Ortiz-López R, Rojas-Martínez A. Ionizing radiation-induced DNA injury and damage detection in patients with breast cancer. *Genet Mol Biol* 2015;38(4):420–432.
- [25] Malkova A, Haber JE. Mutations arising during repair of chromosome breaks. *Annu Rev Genet* 2012;46:455–473.
- [26] Azzam EI, Jay-Gerin JP, Pain D. Ionizing radiation-induced metabolic oxidative stress and prolonged cell injury. *Cancer Lett* 2011;327(1-2):48–60.
- [27] Gong L, Zhang Y, Liu C, et al. Application of radiosensitizers in cancer radiotherapy. *Int J Nanomedicine* 2021;16:1083–1102.
- [28] Kawane K, Motani K, Nagata S. DNA degradation and its defects. *Cold Spring Harb Perspect Biol* 2014;6(6):a016394.
- [29] Sharma BR, Karki R, Kanneganti TD. Role of AIM2 inflammasome in inflammatory diseases, cancer and infection. *Eur J Immunol* 2019;49(11):1998–2011.
- [30] Fernandes-Alnemri T, Yu JW, Datta P, et al. AIM2 activates the inflammasome and cell death in response to cytoplasmic DNA. *Nature* 2009;458(7237):509–513.
- [31] Hornung V, Ablasser A, Charrel-Dennis M, et al. AIM2 recognizes cytosolic dsDNA and forms a caspase-1-activating inflammasome with ASC. *Nature* 2009;458(7237):514–518.
- [32] Hu B, Jin C, Li HB, et al. The DNA-sensing AIM2 inflammasome controls radiation-induced cell death and tissue injury. *Science* 2016;354(6313):765–768.
- [33] Liu M, Xiong Y, Shan S, et al. Eleutheroside E enhances the long-term memory of radiation-damaged *C. elegans* through G-protein-coupled receptor and neuropeptide signaling pathways. *J Nat Prod* 2020;83(11):3315–3323.
- [34] Zhou HC, Sun YY, Cai W, et al. Activation of β 2-adrenoceptor enhances synaptic potentiation and behavioral memory via cAMP-PKA signaling in the medial prefrontal cortex of rats. *Learn Mem* 2013;20(5):274–284.
- [35] Chen Z, Zhong Y, Chen J, et al. Disruption of β -catenin-mediated negative feedback reinforces cAMP-induced neuronal differentiation in glioma stem cells. *Cell Death Dis* 2022;13(5):493.
- [36] Elliott T. Dynamic integrative synaptic plasticity explains the spacing effect in the transition from short- to long-term memory. *Neural Comput* 2019;31(11):2212–2251.
- [37] Saura CA, Cardinaux JR. Emerging roles of CREB-regulated transcription coactivators in brain physiology and pathology. *Trends Neurosci* 2017;40(12):720–733.
- [38] Gordon JN, Prothero JD, Thornton CA, et al. CC-10004 but not thalidomide or lenalidomide inhibits lamina propria mononuclear cell TNF- α and MMP-3 production in patients with inflammatory bowel disease. *J Crohns Colitis* 2009;3(3):175–182.
- [39] Wang M, Li Y, Su J, et al. Protective effects of 4-geranyloxy-2,6-dihydroxybenzophenone on DSS-induced ulcerative colitis in mice via regulation of cAMP/PKA/CREB and NF- κ B signaling pathways. *Phytother Res* 2022;37(4):1330–1345.
- [40] Wang ZY, Shang HH, Gou WF, et al. Protective effect of *Camellia nitidissima* Chi on γ rays radiation-induced hematopoietic and gastrointestinal damage. *Acupunct and Herb Med*. 2024;4(4):487–499.
- [41] Liu L, Jiang Y, Steinle JJ. Epac1 and PKA agonists inhibit ROS to reduce NLRP3 inflammasome proteins in retinal endothelial cells. *Mol Vis* 2022;28:500–506.
- [42] Shi FL, Ni ST, Luo SQ, et al. Dimethyl fumarate ameliorates autoimmune hepatitis in mice by blocking NLRP3 inflammasome activation. *Int Immunopharmacol* 2022;108:108867.